Conditional Simulation of Subseismic Mega-Karstic Features

Amir H. Hosseini and Clayton V. Deutsch

The prediction of the location and size of mega-karstic features such as sinkholes and caves in carbonate reservoirs is important due to their influence on the quality of the reservoirs. Seal effectiveness issues, enhancement of permeability below these features and the potential to be thief zones in thermal recovery applications are among the most important potential impacts on production in carbonate reservoirs. Data collected by seismic surveys can be effectively used to determine the size and shape of the mega-karstic features; however, the only information regarding subseismic features is the knowledge of regional geology and observations at the well locations. This lack of information creates large uncertainties in the intensity, shape, size and location of these features. This paper documents a probabilistic object-based modeling approach for the simulation of location and size of sinkholes. First, uncertainty in the total volumetric proportion of the mega-karstic features is characterized for a site-specific well arrangement. Then, multiple realizations of mega-karstic features are generated while honoring the well data, total volumetric proportions, areal proportion maps and size distributions. The parameterization of the shapes of sinkholes is based on three-dimensional hemi-ellipsoidal shapes. The sequential placement is carried out by adapting a Gaussian function based on the areal proportion maps and drawing from an updating cumulative distribution function.

1. Introduction

The upper Devonian Grosmont formation in northern Alberta is a carbonate platform complex that was exposed for a long period of time between the Mississippian and Cretaceous. A widespread karst system is developed in this exposure period and is characterized by an irregular erosional surface (unconformity), dissolution cavities, collapsed breccias, sinkholes and fractures. These paleokarst features in the Grosmont formation are more common in the upper units and the effects of karstification decrease toward stratigraphically older and deeper units. According to Dembicki and Machel (1996), the paleokarst usually occurs within 35 m of the unconformity. Karstification significantly influences reservoir properties such as thickness, porosity, permeability and the seal effectiveness between upper and lower units (upper and lower Grosmont formation). Karstification can either benefit or degrade reservoir characteristics; large porosity and permeability values can be found at the fracture locations or immediately below the mega-karstic features, while seal effectiveness is reduced and the existence of thief zones at mega-karst locations are detrimental for thermal recovery applications. The focus of this paper is on presenting a new statistical methodology for characterizing the uncertainty in the distribution of sinkholes that are discrete features and can be modeled as a Poisson point processes.

The origins of modern karst features and their internal structure are well documented (Loucks 1999 and Loucks and Mescher 2001). Loucks (1999) used a ternary diagram to define caves, sinkholes, sediment fills and breccias. In their work, Loucks (1999) also described the processes by which a modern cave passage is a product of near-surface karst processes that include the dissolutional excavation of the passage with partial to total breakdown of the passage and sedimentation (Figure 1). In another work, Loucks and Mescher (2001) proposed a classification of six common paleokarst facies. More specifically, post-depositional alteration of regional dip due to internal erosion and deformational processes caused by subsurface karstification of carbonates or evaporates result in the formation of sinkholes. Among the most common processes involved in the generation of the sinkholes include brittle gravitational deformation of cover and rock material (collapse), downward migration of cover material through dissolutional conduits and its progressive settling (suffusion), and ductile flexure of rock formations (sagging) (Williams 2004, Galve et al. 2009).

Although the origin, the evolution and the internal structure of paleokarst features in general and sinkholes in particular are well-studied, the information available about paleokarst hydrocarbon reservoirs at the interwell scale is limited. The available information for characterization of geometry and spatial distribution of mega-karstic features include areal seismic survey data as well as observations at the wells. There are a number of works in the literature that have used seismic data to deterministically characterize the size and location of these features (Majcher et al. 2005, Shen et al. 2007 among others). In a heavy oil field (Bakken Sand Pool Court field) in west-central Saskatchewan, Majcher et al. (2005) observed that the lateral continuity of the sand ridge is variable

due to post-depositional sinkholes. This structural complexity based on 3D seismic and well-logs were deterministically incorporated into the reservoir model. It was observed that the sinkholes vary greatly in size and shape, and their identification was limited by the seismic resolution of the surveys. The lower limit of horizontal resolution of the sinks was between 45 to 60 m. Similarly, Shen et al. (2007) presented an integrated approach to incorporate processed seismic geometric attributes, lithofacies, well log and drilling data into imaging karst networks and characterizing their effective properties in Ordovician carbonate reservoirs. In their work, they used dip maps to identify the sinkholes and deterministically locate them in the reservoir model. Similar to the work of Majcher (2005), the identification of the paleokarst features was limited by seismic resolution. Previous research into statistical modeling of frequency, size and shape of sinkholes is limited. Previous researches in this area include some works in the areas of urban development hazard assessment (Weltham et al. 2005, Gutierrez et al. 2008, Galve et al. 2009) where development of susceptibility maps (spatial probability of sinkholes) and hazard maps (spatio-temporal probability of sinkholes) is studied, as well as subsidence simulations for abandoned mines (Park and Li, 2004, and Choi and Deb 2005), where a number of analytical and numerical (fuzzy reasoning) approaches have been proposed based on rock mechanical properties and mine gallery opening, among other factors. As pointed out by Galve et al. (2009) and Choi and Deb (2005), the quality of the predictive models will depend to a great extent on the completeness and representativity of the sinkhole inventory and the correlation of its probability of occurrence with model parameters, which is largely inaccessible for subsurface systems.

For carbonate reservoirs and at sub-seismic resolution, the only available information about the existence of mega-karstic features is the knowledge of regional geology (karstified reservoir, existence of floodplain, etc.) and observations at the well locations. In this paper, we first propose a statistical object-based methodology for simulating sinkholes. An example is presented to show how the volumetric proportion of the primary objects (sinkholes) is characterized. Objects are simulated for two different areal proportion maps (APMs), and the reproduction of basic statistics such as the distribution of volumetric proportion and sizes are checked.

2. Methodology

The proposed methodology is based on first characterizing the uncertainty in the total volumetric proportion of the primary objects (sinkholes) in the reservoir and then sequentially simulating these objects, while honoring well observations and volumetric proportions. Inputs to the methodology are the layout and depth of the existing wells, APMs, obtained based on regional geology and parameterization of the shape of the primary objects. The output of the methodology are realizations of sinkholes that can be super-imposed into geological models of the reservoir for subsequent ranking and flow simulation. Figure 2 shows the workflow for the proposed methodology.

According to Figure 2 the first steps in the methodology are related to parameterization of shape and size of the primary objects, calculation of the distribution of volumetric and observed longitudinal proportions and updating APMs. In general, Boolean models depend on two parameters: the intensity of the Poisson point process and the probability distribution of the primary objects (Chiles and Delfiner 1999). The intensity of the point process is closely related to areal/vertical proportion maps. The probability distribution of the primary objects is related to the volumetric proportions and the size and geometry of the primary objects. As discussed above, the geology of the Grosmont formation suggests that sinkholes exist in the upper layers of the Grosmont formation exposed to the unconformity. Thus, the examples shown below are based on modeling sinkholes immediately below the unconformity. The presented methodology is general and can be directly used for modeling other mega-karstic features. Any level of complexity can be incorporated into the parameterization of shapes of the mega-karstic features. Based on the observations of the outcrops (USGS website accessed 27/10/09), a semi-ellipsoidal shape parameterized by the length of its first major axis, horizontal and vertical aspect ratios and the azimuth of its first major axis has been adapted in the work. Figure 3 shows the proposed parameterization for the shape of the primary objects, where d, AR_H and AR_V are the radius, and horizontal and vertical aspect ratios. In the proposed methodology, all of these parameters have Gaussian distributions and are independent. The independency of the size and direction distributions creates variety of different shapes and sizes in each realization. It should be noted that all the workflow is performed after transformation of reservoir units into stratigraphic units. Another important primary step is to establish the APM based on an understanding of geology of the reservoir and an associated updating scheme. Based on the outcrops in central Florida and Mexico (USGS website accessed 27/10/09), overlapping of primary objects are expected to be small. Thus, an updating scheme is defined to adequately account for repulsion effects in simulating successive primary objects in each realization. Figure 4 depicts the parameterization of the updating scheme for areal proportion maps. A Gaussian model has been used

to update the intensity map (APM) upon insertion of new objects in the system. The updating model is similar to a Gaussian variogram model and represented by:

$$\mathrm{I}^{new}(\mathbf{d}) = \begin{cases} \mathrm{I}^{old}(\mathbf{d}) + (1 - c_0).\exp\left(-\dfrac{9(\mathbf{d}-\mathbf{r})^2}{a^2}\right) & , \ \mathbf{d} \geq \mathbf{r} \\ c_0 & , \ \mathbf{d} < \mathbf{r} \end{cases} \quad [1]$$

where, **d** is the distance to the center of the ellipsoid, c_0 is the nugget constant that is set to a small value to ensure that minimal overlapping occurs after placing subsequent objects, **r** is the directional polar of the ellipsoid (Figure 3), *a* is the range of updating Gaussian model that can be considered proportional to the size of the first major axis of the ellipsoid, and I^{old} and I^{new} are the values of the intensity map before and after updating. The range of the updating model is the primary factor controlling the distance between subsequent objects. Figure 5 shows a few planar snapshots of the updating (initially uniform) APM with a range equal to three times the size of each primary object. The location of each subsequent primary object is randomly drawn after transforming the APM to a cumulative distribution function (CDF) to provide control over the distance of the objects.

Simulating multiple realizations of distribution of sinkholes for different total volumetric proportions and calculating the observed 1D proportion at the wells, one can construct the bivariate relationship between total volumetric proportions and the observed 1D proportion (the first major step in the workflow in Figure 2). As shown in the subsequent example, this bivariate relationship can be used to characterize the uncertainty in the volumetric proportions for every given well arrangement. The second major step of the methodology involves simulating the primary objects. A stratified simulation is adapted, that is, primary objects are first simulated at the well locations and then at the other locations of the reservoir until the target volumetric proportion is honored. Drawing the size and location of the sinkholes are implemented randomly based on user-defined size distribution and user-defined updating APMs.

A few checks are required: (1) reproduction of the target volumetric proportion histogram over all realizations, (2) for each realization, the reproduction of input size distributions should be checked, and (3) consistency between the location of the simulated sinkholes and the input APM.

3. Example

To characterize the uncertainty in the volumetric proportions and to demonstrate the overall methodology, a synthetic example is presented. The study site is 1 km × 1 km × 50 m with 10 fully-penetrating wells (Figure 6). The red circles in Figure 6 show the location of the wells with observed sinkholes. The observed sinkholes at wells 3 and 9 are assumed to be immediately below the unconformity and their apparent depths are 10.0 m and 16.0 m, respectively. Thus, the observed 1D proportion at the wells is equal to 5.2 percent. Figure 7 shows the reference case. First, a uniform APM has been generated. In order to characterize the uncertainty in the volumetric proportions, 4000 realizations of sinkhole distributions are simulated over a wide range of volumetric proportions. For all the realizations, Gaussian distributions are adapted for the size of the first major axis, horizontal aspect ratio and vertical aspect ratio of the simulated ellipsoids, and a uniform random distribution between 0 and 180° is assumed for the azimuth. Assuming a threshold of 30 m for the areal seismic resolution, Gaussian distributions with means of 16.0 m, 1.0 and 1.0, and standard deviations of 6.0 m, 0.3 and 0.3 are adapted for the size of first major axis and horizontal and vertical aspect ratios, respectively. To maintain minimum overlapping between the simulated objects a very small nugget (~0.001), a horizontal range equal to three times the size of the primary object and vertical range equal to the depth of the primary object are selected. Figure 8 shows the resulting bivariate distribution between 1D observed proportions at the wells and 3D volumetric proportion of simulated sinkholes. The mean and 70 percent confidence interval, as well as the arrow marking the reference 1D proportion are shown. Figure 9 shows the histogram of the volumetric proportions corresponding to the reference 1D proportion of 5.2 percent. The bivariate distribution and the histogram in Figures 8 and 9 are based on a uniform APM. As it can be observed in the outcrop in the areal photo from central Florida shown in Figure 10 (top), there can be a trend in the occurrence of the sinkholes. Thus, to investigate the effects of a non-uniform APM, the channelized APM in Figure 10 (right) is considered and used in characterizing the uncertainty in the volumetric proportions and subsequent simulation of object-based realizations. Figures 11 and 12 show the bivariate distribution between volumetric and 1D proportions, and the histogram of the volumetric proportions for the reference 1D proportion, for the channelized APM. Comparing Figures 8, 9, 11 and 12, one can observe that

adapting different APMs has minimal impact on the bivariate distribution of 1D and 3D proportions, and the histogram of volumetric proportions for the reference 1D proportion. The calculated histograms (Figures 9 and 12) together with size and shape distributions and APMs are input to the next step of the proposed methodology, that is, simulation of primary objects and generating multiple realizations. For uniform and channelized APMs, Figures 13 and 14 show four realizations of the distribution of the primary objects for the two different APMs. It can be observed that all realizations honor the observation of the sinkholes at the well locations and follow the trend observed in the APMs. Figures 15 and 16 show the reproduction of size distributions (the size of the first major axis) for the four realizations. Figure 17 shows the reproduction of the distribution of volumetric proportions over 200 realizations. Figures 15 to 18 show good reproduction of input statistics. Similarly, it can be shown that the input distributions for the second major axis, depth and azimuth are reproduced for all generated realizations.

As stated previously, the realizations can be incorporated into individual realizations of geological models of carbonate reservoirs to represent mega-karstic features. The assignment of facies type to these features can be based on recognizing one or multiple facies types (Figure 1). Assignment of properties with a simulation algorithm, such as sequential Gaussian simulation, to the facies types would provide the final static reservoir model. Ranking can be used to select a subset of models for further flow simulation analysis to assess the impact of karstic features on reservoir performance.

4. Conclusions

The authors have proposed a conditional object-based modeling approach for characterizing the uncertainty in spatial distribution of sub-seismic mega-karstic features in carbonate reservoirs. The proposed technique is based on the incorporation of the relationship between 1D observed proportions at the well locations and 3D true volumetric proportions of the karstic features (and its associated uncertainty) in the reservoir. The parameterization of the shape of the features is in the form of hemi-ellipsoids with different size, aspect ratio and orientation; and the spatial distribution of the features is controlled by the hard data at the wells, areal proportion maps and the volumetric proportion of the features and associated uncertainty. Multiple conditional realizations of mega-karstic features are generated that can be used in reservoir characterization workflow for subsequent uncertainty assessment. The proposed technique shows good reproduction of the distribution of volumetric proportions, size parameter distributions and APMs.

References

Choi, S.O., Deb, D. Fuzzy analysis on subsidence occurrences at abandoned mine area; *Proceedings of Alaska Rocks, the 40th U.S. symposium on Rock Mechanics: Rock Mechanics for Energy, Mineral and infrastructure development in the northern regions, June 25-29 2005, 7 p., ARMA # 05-728*

Dembicki, E.A., Machel, H.G., Recognition and delineation of paleokarst zones by the use of wireline logs in the bitumen-saturated Upper Devonian Grosmont Formation of northeastern Alberta, Canada; *AAPG Bulletin, 1996, v. 80, no. 5, p. 695-712*

Galve, J.P. et al., Probabilistic sinkhole modeling for hazard assessment; *Journal of Earth Surface processes and Landforms, 2009, vol. 34, p. 437-452*

Gutiérrez F., Cooper A.H., Johnson K.S., Identification, prediction and mitigation of sinkhole hazards in evaporite karst areas; *Environmental Geology, 2008, vol. 53, p. 1007–1022.*

Loucks, R. G., Paleocave carbonate reservoirs: origins, burial depth modifications, spatial complexity, and reservoir implications; *AAPG Bulletin, 1999, v. 83, p. 1795– 1834*

Loucks, R. G., Mescher, P.K., Paleocave facies classification and associated pore types in A geologic odyssey; *AAPG Southwest Section Annual Meeting, Dallas, Texas, March 11–13, 2001, 18 p.*

Majcher, M.B., Estrada, C.A., Archer, J.C., Evaluation of the potential for reduction in well spacing of the Bakken sand pool, court field; *Proceedings of the SPE international Thermal Operations and Heavy Oil symposium, Calgary, AB, 1-3 November 2005, 19 p., SPE # 97741*

Shen, F., Qi, L., Han, G., Characterization and Preservation of Karst Networks in the Carbonate Reservoir Modeling; *Proceedings of SPE Annual Technical Conference and Exhibition, Anaheim, CA, 11-14 November 2007, 8 p., SPE # 110072*

Waltham T., Bell F., Culshaw M., *Sinkholes and Subsidence; Springer: Berlin, 2005.*

Williams P., Dolines; *In Encyclopedia of Caves and Karst Science, Gunn J (ed.). Taylor and Francis, New York, 2004, p. 304–310*

Figures

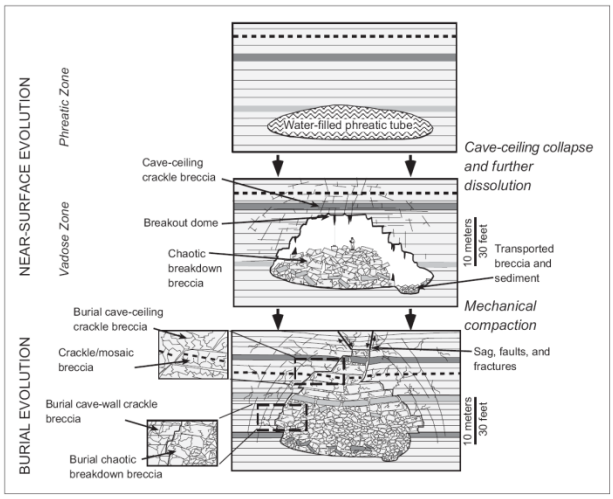

Figure 1: The evolution of a single cave passage from its formation in the pheretic zone to burial in the subsurface (Loucks 1999).

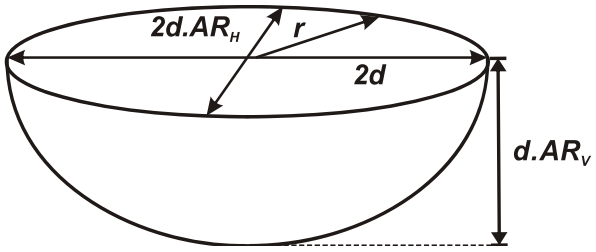

Figure 3: Parameterization of shape of the objects as a hemi-ellipsoid with its major axis, horizontal and vertical aspect ratios, and azimuth.

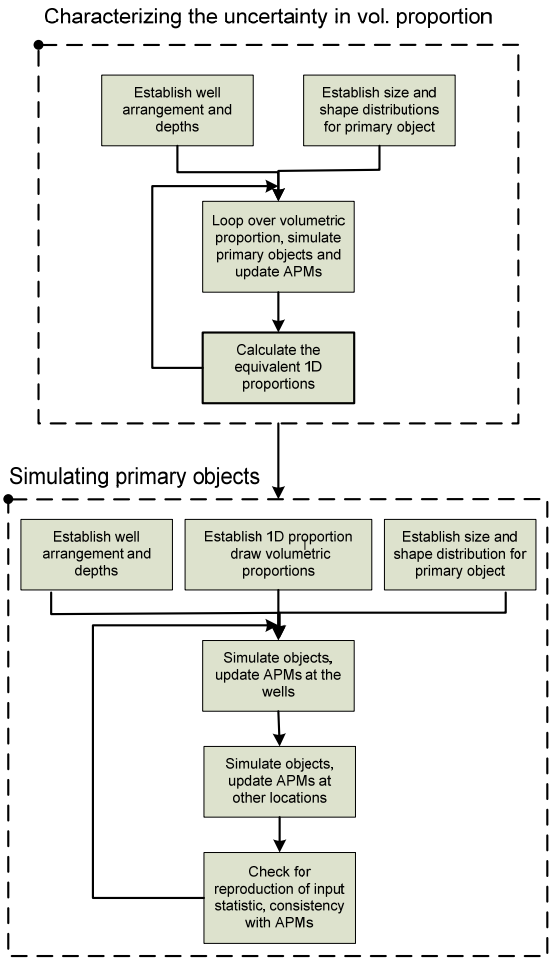

Figure 2: Workflow for the proposed object-based modeling technique for (1) characterization of uncertainty in volumetric proportions, and (2) simulating primary objects, honoring the well data, areal proportion maps, and proportion and size distributions.

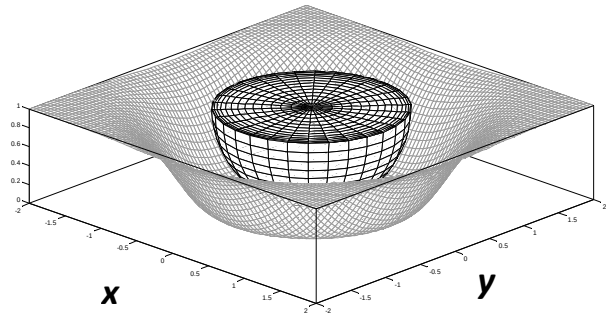

$1 - \Delta I$

Figure 4: Parameterization of updating function for intensity (areal proportion) map to ensure minimal overlapping of subsequent objects (repulsion effect).

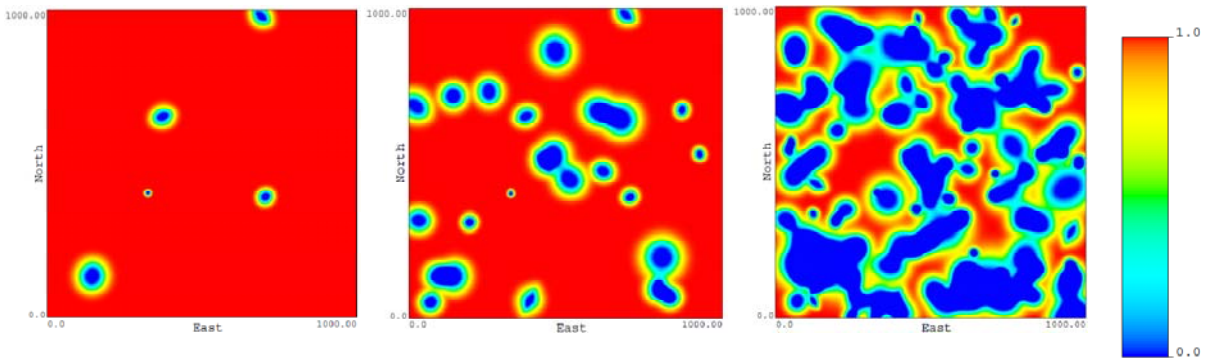

Figure 5: Evolution of the areal proportion map after inserting multiple primary objects.

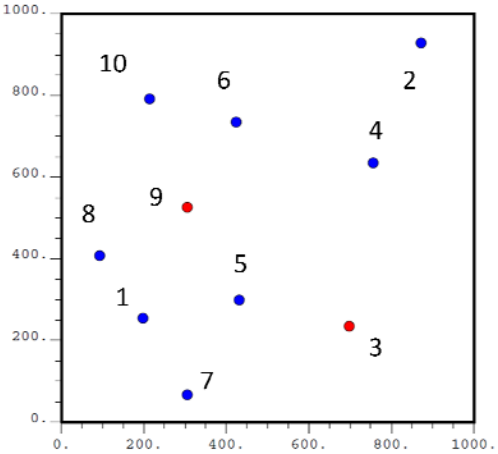

Figure 6: The location map for the wells in the synthetic example. The red circles show the location of wells with the observed mega-karst features.

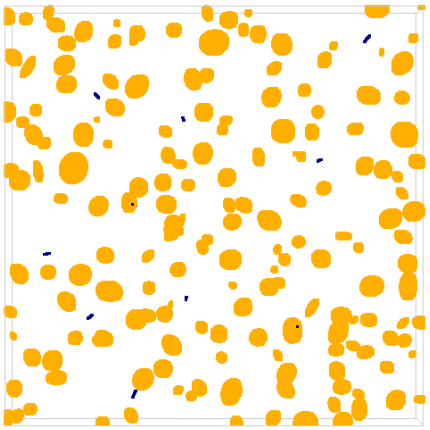

Figure 7: The reference distribution of the sinkholes in the 3D domain. The observed 1D proportion is equal to 5.2 percent and the true total volumetric proportion is equal to 3.6 percent.

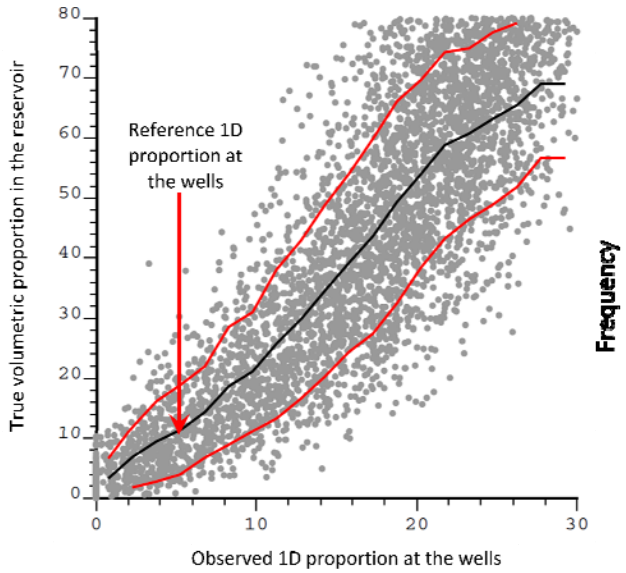

Figure 8: The bivariate distribution between the total volumetric distribution and the observed 1D proportion at the well locations for a uniform APM.

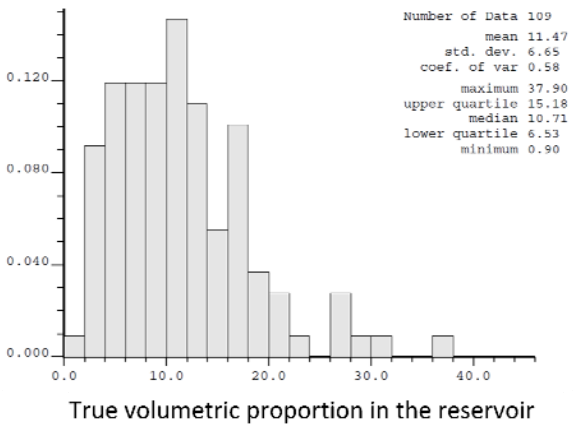

Figure 9: The histogram of the true volumetric proportion for the reference length proportion, for a uniform APM.

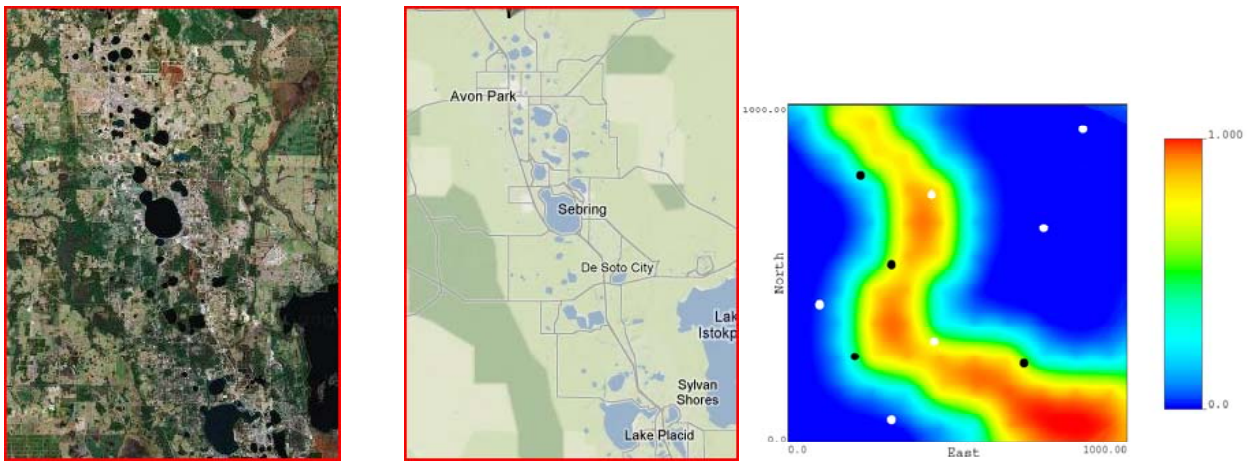

Figure 10: A satellite photo (left) and terrain map (middle) from central Florida (Lat: 27.5070, Long: -81.4038) showing a trend (floodplain) in occurrence of the sinkholes, and a hypothetical APM showing a channelized trend in occurrence of the sinkholes (right).

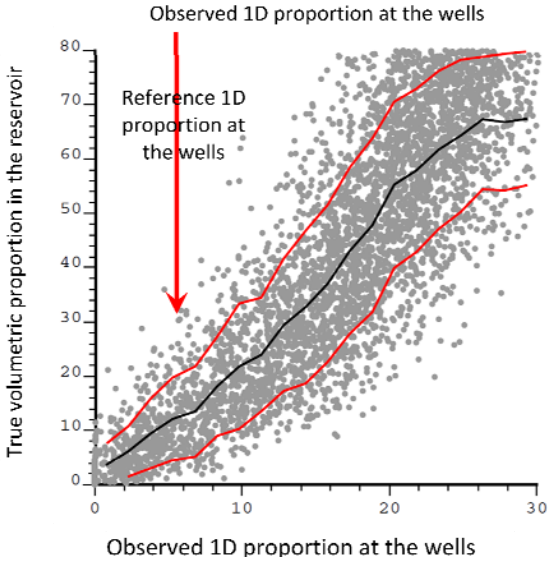

Figure 11: The bivariate distribution between the total volumetric distribution and the observed 1D proportion at the well locations for a channelized APM.

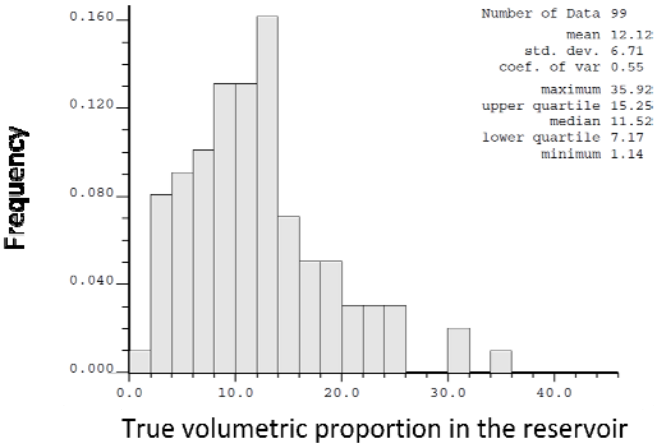

Figure 12: The histogram of the true volumetric proportion for the reference length proportion, for a channelized APM.

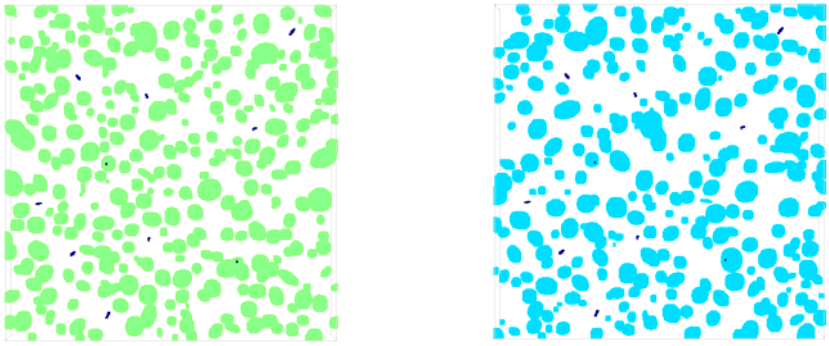

Figure 13: Two realizations of sinkhole distributions based on a uniform APM. Reproduction of well observations and uniform distribution of sinkholes can be noticed.

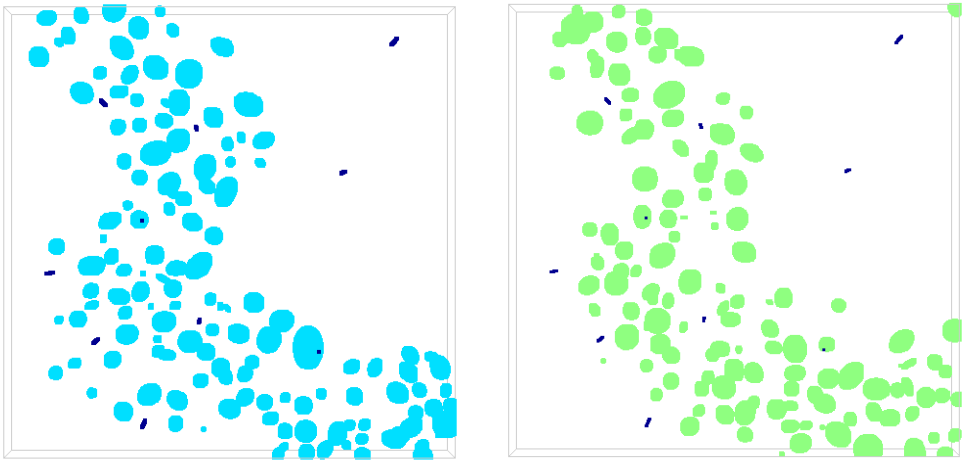

Figure 14: Two realizations of sinkhole distributions based on a channelized APM. Reproduction of well observations and uniform distribution of sinkholes can be noticed.

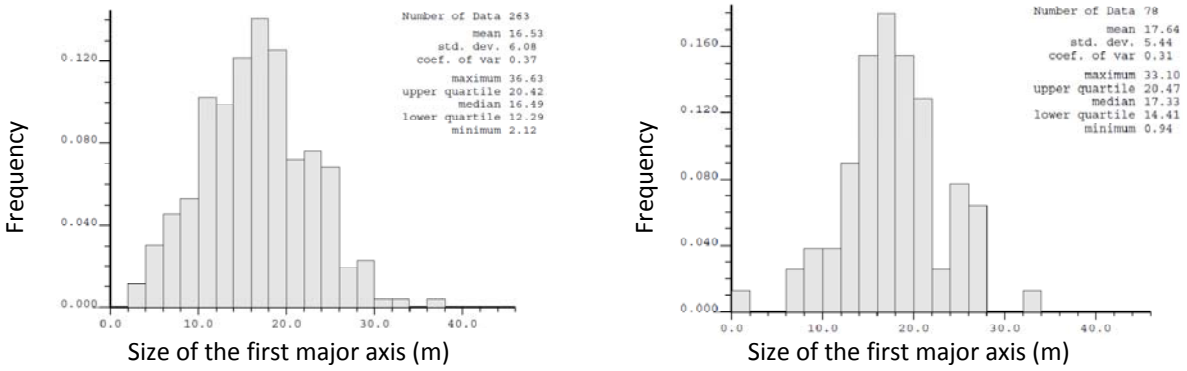

Figure 15: Reproduction of the size distributions for the two realizations of sinkhole distributions based a uniform APM.

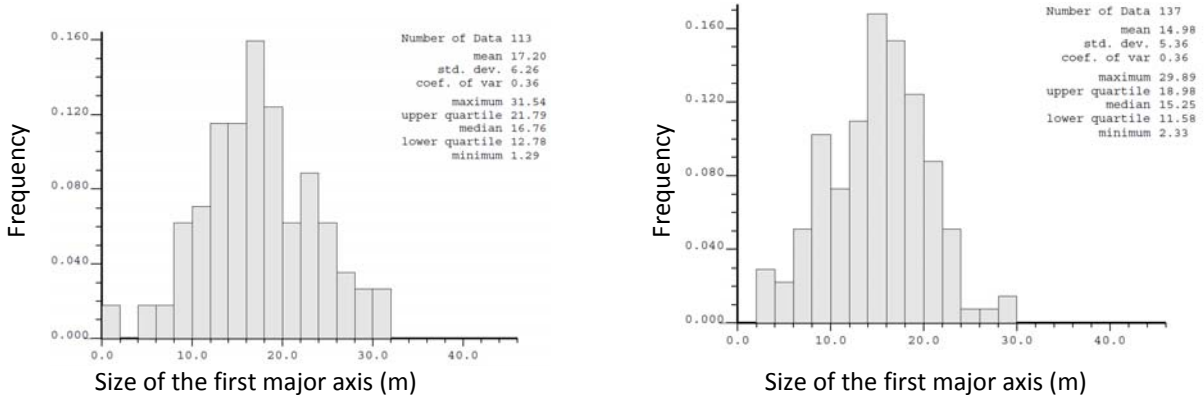

Figure 16: Reproduction of the size distributions for the two realizations of sinkhole distributions based a channelized APM.

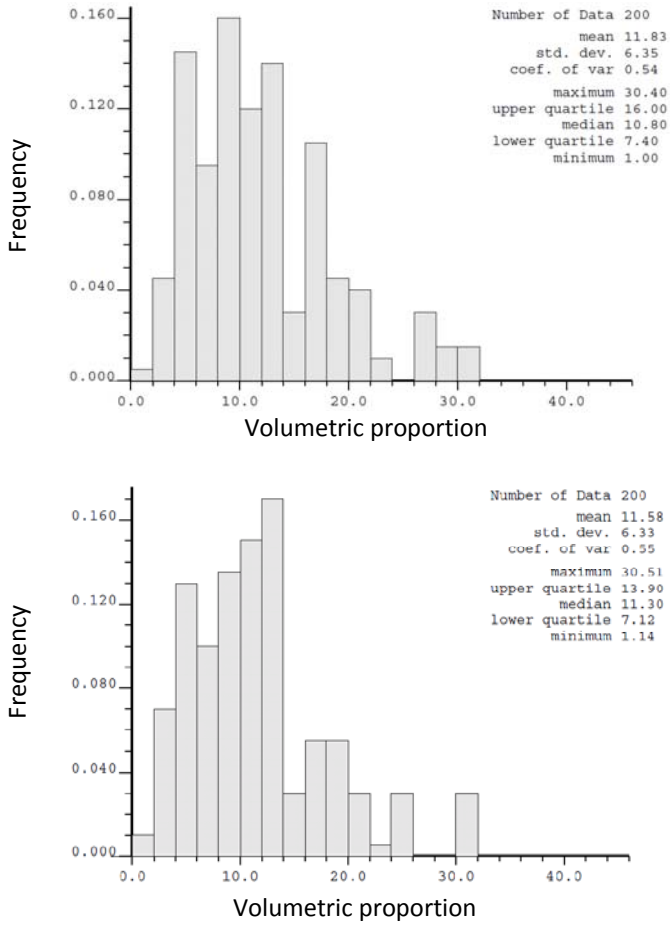

Figure 17: Reproduction of the input volumetric proportions over ensemble of 200 realizations based a uniform APM (up) and a channelized APM (down).